Transient behavior of the second-order optical process in $Cd_xZn_{1-x}Te$: Transformation from luminescence into Raman scattering

A. Nakamura,* M. Shimura, and M. Hirai
Department of Applied Physics, Faculty of Engineering, Tohoku University, Sendai, Miyagi 980, Japan

M. Aihara
Department of Physics, Faculty of Liberal Arts, Yamaguchi University, Yamaguchi 753, Japan

S. Nakashima
Department of Applied Physics, Faculty of Engineering, Osaka University, Suita, Osaka 565, Japan
(Received 7 July 1986; revised manuscript received 8 September 1986)

We report on the transient behavior of the second-order optical process in the picosecond time region in mixed semiconducting crystals. Time-integrated spectra under resonant excitation below the band gap exhibit "Raman-like" lines associated with localized excitons. However, time-resolved spectroscopy enabled us to resolve these Raman-like lines into resonant luminescence and Raman scattering lines. We have found the transformation of luminescence into Raman scattering as a function of incident frequencies without changing the spectral shape. Furthermore, the intensity ratio between Raman scattering and luminescence was determined for a wide range of the off-resonance frequency. The result is unambiguously explained by the theory by taking into account the finiteness of the correlation time of the reservoir. This gives the first experimental evidence for the non-motional-narrowing effect in the second-order optical process.

I. INTRODUCTION

When the crystal or the vapor is excited by the short light pulse whose frequency ω_i is tuned to the transition frequency ω_0 between a ground and an excited state, the time response of the secondary emission is governed by the lifetime of the excited state. This second-order optical process is interpreted simply by absorption followed by luminescence. However, when ω_i is moved away from resonance, the time the system can spend in its excited state is limited to the inverse of the frequency difference Δ_c^{-1} between ω_i and ω_0 because of the uncertainty relation. Such transient behavior of the secondary emission intensity has recently received considerable interest and has been both experimentally[1-3] and theoretically[4-7] investigated by several workers. In an experimental study, Williams *et al.*[1] have performed direct measurements of the time response of the secondary emission in I_2 vapor. They demonstrated that the long-lived exponential decay was observed when ω_i was on resonance while the time response became very fast when ω_i was slightly moved off-resonance. Such a transition from resonance fluorescence to resonant Raman scattering (RRS) was studied also theoretically within the framework of the fast modulation limit, i.e., motional-narrowing limit.[4,5] They succeeded to explain the transition from luminescence into RRS near resonance. However, these theories indicate that even at large off-resonance, the luminescence component remains constant and the second-order optical process does not completely transform into ordinary Raman scattering (RS). Hence, these studies are not applicable to the transient and spectral behavior of the second-order optical process in the wide range of ω_i from resonance to large off-resonance.

If ω_i is moved off far from resonance, the time Δ_c^{-1} becomes comparable to the correlation time τ_c of the reservoir. In this regime, the memory effect of the reservoir should play an important role during the course of the dissipative process in the second-order optical process. Recently, Aihara[7] has developed a theory of transient behavior of the second-order optical process taking into account the finiteness of τ_c in the dissipative processes. The concept of the motional narrowing in which the constant rate of the transverse relaxation can describe the relaxation phenomena is no more valid in this regime. Hence, this memory effect can be called a "non-motional-narrowing effect" due to the finiteness of τ_c. He demonstrated that this effect suppresses considerably the contribution of the luminescence component at large off resonance, and revealed the important role of the memory effect.

In this paper we report the first experimental evidence for the importance of the non-motional-narrowing effect when the second-order optical process approaches the nonresonant regime. The study by time-resolved spectroscopy was performed on the excitonic system with large inhomogeneous broadening in $Cd_xZn_{1-x}Te$ mixed crystals. The time-resolved spectroscopy enabled us to discriminate between luminescence and RS components in the secondary emission. The continuous transition of RRS into resonant luminescence as a function of ω_i has been reported in a previous paper.[3] In the present work, however, we have performed the measurement of off-resonant behavior in the wide range of Δ_c. The detailed analysis of the results allowed us to determine the intensity ratio of resonant luminescence to the total secondary emission as a function of Δ_c. In contrast to the results in I_2 vapor, the observed ratio is unambiguously explained by the theory

of transient second-order optical process, taking into account the finiteness of τ_c.

In the following section we present the theory for the transient resonant light scattering, taking into account the finiteness of τ_c. We describe our experimental procedure and results of spectral and temporal behavior of the secondary emission from the exciton system in $Cd_xZn_{1-x}Te$ ($x=0.32$) in Secs. III and IV. In Sec. V we will analyze the intensity ratio of luminescence to the total secondary emission as a function of Δ_c by the theory of Sec. II. Origin of the phase relaxation process for the exciton system in the mixed crystal is also discussed on the basis of the temperature dependence of the intensity ratio observed.

II. THEORY

In this section we present the theoretical background for the transient resonant light scattering with emphasis on the non-motional-narrowing effect which is caused by the finiteness of the reservoir correlation time τ_c. As pointed out recently by one of the present authors,[7] the finiteness of τ_c gives rise to the reduction of the intensity ratio of the luminescencelike slow component to the scatteringlike rapid component. This effect becomes significant, especially in the condensed matter with large inhomogeneous broadening comparable to $\hbar\tau_c^{-1}$. The non-motional-narrowing effect is important even if τ_c is much less than the inverse of the system-reservoir coupling strength D^{-1}, which is the usual motional-narrowing condition. This theory first explained the transition from the luminescencelike process in the exact resonance to the scatteringlike process in the far off-resonance. The mixed crystal with the large inhomogeneous broadening due to the disorder will be a good example for observing the predicted non-motional-narrowing effect.

The time dependence of the secondary emission can be generally expressed by[6]

$$I(t)=\int_{-\infty}^{t}dt_1\int_{-\infty}^{t}dt_2\,F_i(t_1)F_i(t_2)g(t_1-t_2)\times\exp[i\Omega_i(t_2-t_1)-(\gamma/2)(2t-t_1-t_2)]\,, \tag{1}$$

where Ω_i is the mean frequency of incident photon, $F_i(t)$ the pulse shape of the incident light, and γ^{-1} the lifetime of the excited state. Within the second comulant, $g(t)$ is given by the following form:

$$g(\sigma)=\exp(i\epsilon\sigma)f(\sigma)\,, \tag{2}$$

$$f(\sigma)=\exp\left[-\int_0^{\sigma}ds_1\int_0^{s_1}ds_2\langle V(s_1)V(s_2)\rangle\right]. \tag{3}$$

Here, $V(t)$ denotes the system-reservoir interaction in the interaction picture and we assume the correlation function has the form

$$\langle V(s_1)V(s_2)\rangle=D^2\exp(-|s_1-s_2|/\tau_c)\,, \tag{4}$$

where the correlation time τ_c is of the order of the inverse of the reservoir spectral width and D is the measure of the system-reservoir coupling strength. With use of the above form, Eq. (3) becomes

$$f(\sigma)=\exp\{-D^2\tau_c[\sigma-\tau_c(1-e^{-\sigma/\tau_c})]\}\,. \tag{5}$$

Assuming the Gaussian form for both the incident pulse shape and for the inhomogeneous broadening, we obtain

$$I_i(t)=\int_0^{\infty}d\sigma\exp[(\gamma/2\delta)^2-\gamma t-(\delta_i^2+\delta^2)\sigma^2/4]\times f(\sigma)\cos(\Delta_c\sigma)\times E_{rfc}[-\delta(t-\sigma/2-\gamma/2\delta^2)]\,, \tag{6}$$

where Δ_c is the off-resonance frequency, δ the spectral width of the incident light, and δ_i the inhomogeneous spectral width. The above equation indicates that the scatteringlike component, which follows the incident pulse shape, and the luminescencelike component, which decays with the lifetime of the excited state, appear. The luminescencelike part is obtained by

$$I_L(t)=C\int_{-\infty}^{t}d\tau\exp[-\delta^2\tau^2-\gamma(t-\tau)]\,. \tag{7}$$

The coefficient C in the above equation should be determined so as to satisfy $I_L(t\gg\delta^{-1})=I_i(t\gg\delta^{-1})$ and we find

$$C=2(\delta/\pi^{1/2})\int_0^{\infty}d\sigma\exp[-(\delta_i^2+\delta^2)/4]f(\sigma)\cos(\Delta_c\sigma)\,. \tag{8}$$

Therefore, Eq. (7) becomes

$$I_L(t)=E_{rfc}[-\delta(t-\gamma/2\delta^2)]\times\int_0^{\infty}d\sigma\exp[(\gamma/2\delta)^2-\gamma t-(\delta_i^2+\delta^2)/4]\times f(\sigma)\cos(\Delta_c\sigma)\,. \tag{9}$$

The time-integrated intensity for the luminescence component (7) and that for the total secondary emission (6) are given as follows:

$$I_L=\gamma^{-1}\int_0^{\infty}d\sigma\cos(\Delta_c\sigma)\exp[-(\delta_i^2+\delta^2)(\sigma/2)^2]f(\sigma)\,, \tag{10}$$

$$I_{\rm tot}=\gamma^{-1}\int_0^{\infty}d\sigma\cos(\Delta_c\sigma)\times\exp[-(\gamma/2)\sigma-(\delta_i^2+\delta^2)(\sigma/2)^2]f(\sigma)\,. \tag{11}$$

It should be noted that in the large off-resonance frequency where Δ_c is comparable to τ_c^{-1}, the deviation of $f(\sigma)$ from the form $\exp(-D^2\tau_c\sigma)$ due to the finiteness of τ_c in Eq. (5) causes the reduction of the luminescence fraction. Since the system cannot stay in its excited state longer than the Δ_c^{-1} because of the energy-time uncertainty relation, the finiteness of τ_c takes part in the problem even for $\tau_c\ll D^{-1}$.

Now let us consider the microscopic origin of the phase relaxation for the exciton system in mixed crystals. One of the possible mechanisms is the exciton-phonon interaction. In this case, the interaction

$$V(t)=\exp(iH_0t)V\exp(-iH_0t)$$

(H_0 is the free part of the exciton-phonon Hamiltonian) is the function of the fluctuating phonon field and τ_c is of the order of the inverse of the width of the phonon densi-

ty of states. The other possible dephasing mechanism is due to the substitutional disorder in mixed crystals. In this case, V denoted the spatial potential fluctuations and H_0 denotes the exciton Hamiltonian for the perfect crystal. Since H_0 does not commute with V, $V(t)$ fluctuates in time. As a result, the excitons feel the fluctuating environment and τ_c is of the order of the inverse of the exciton bandwidth. In the case of Wannier excitons with a large orbital, the fluctuations which the excitons feel are the spatially averaged ones, so that the fluctuation process may be approximately regarded as the Gaussian-Markov process. More rigorous treatment for the Frenkel excitons based on the coherent-potential approximation has been performed by one of the present authors.[8]

III. EXPERIMENT

The experiment was performed by using a synchronously mode-locked dye laser and a time-correlated single-photon counting method. The spectral and the temporal widths of the mode-locked pulse were about 7 cm^{-1} and 10 ps, respectively. The full width at half maximum of the time response of the measuring system was 350 ps for the laser pulse. The time resolution of about 50 ps was obtained for decay curves by using a convolutional analysis. The secondary emission from the (110) surface of the crystal was collected by the backward-scattering geometry. The spectrum was analyzed by a double monochromator equipped with a cooled photomultiplier. The $Cd_xZn_{1-x}Te$ crystals used in this work were grown in Te-excess solution by the Bridgman method. The surfaces were etched in 20% aqueous solution of NaOH at 50—60 °C. The size of the sample was $3.5\times3.0\times2.5$ mm^3, so that the thickness was always larger than the penetration depth of light in the range of the incident frequency under study.

IV. EXPERIMENTAL RESULTS

Figure 1 shows a luminescence spectrum (a) observed by the band-to-band excitation at 514.5 nm and a series of secondary emission spectra (b)—(f) by the resonant excitation near the main luminescence bands at 1.8 K. In spectrum (a), two main luminescence bands are seen; the X band (16 835 cm^{-1}) originates from the mobile excitons and the localized exciton (LE) band (16 790 cm^{-1}) originates from the excitons localized in the tail state as a result of random potential fluctuations due to the local compositional disorder.[9–12] Spectra (b)—(f) represent secondary emission spectra by resonant excitation in the vicinity of X and LE bands. The position of ω_i in each spectrum is indicated by an arrow. The frequency shifts of the LO_1 and LO_2 lines from ω_i are constant and close to the LO-phonon frequencies of pure CdTe and ZnTe crystals, respectively. The shift of the TO_2 line corresponds to TO-phonon frequency of pure ZnTe crystals. The spectral features seen in this figure resemble those of RRS by optical phonons. However, a time response of these lines allowed us to separate the contribution of Raman and luminescence processes to the secondary emission.

These results are clearly displayed in Fig. 2 where decay curves of emission intensity monitored at the peak position of the LO_2 lines are illustrated for various ω_i's. The decay curve (c) for 16 790 cm^{-1} exhibits a single exponential decay, whereas a short-lived component appears in the decay curves for other frequencies in addition to the long-lived component. Calculating decay curves by the convolution of a kinetics function with the instrumental

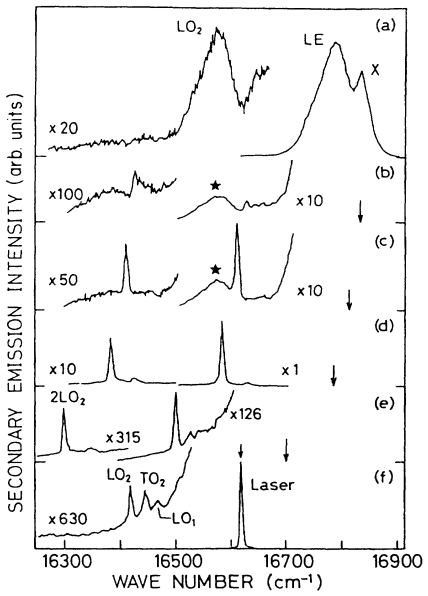

FIG. 1. Secondary emission spectra of $Cd_xZn_{1-x}Te$ ($x=0.32$) at 1.8 K. Incident frequencies: (a) 19 436 cm^{-1}, (b) 16 833 cm^{-1}, (c) 16 817 cm^{-1}, (d) 16 790 cm^{-1}, (e) 16 702 cm^{-1}, (f) 16 621 cm^{-1}.

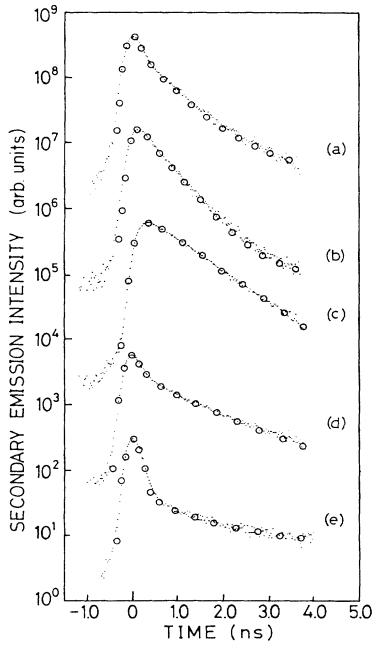

FIG. 2. Decay curves of the secondary emission intensities at the peak position of the LO_2 lines. Incident frequencies: (a) 16 333 cm^{-1}, (b) 16 817 cm^{-1}, (c) 16 790 cm^{-1}, (d) 16 702 cm^{-1}, (e) 16 621 cm^{-1}. The open circles represent the convoluted values.

response, we have obtained decay times for both components. We assumed two exponential functions with τ_R and τ_{L1} for 16 790 and 16 702 cm^{-1} and three exponential functions with τ_R, τ_{L1} and τ_{L2} for 16 833, 16 817, and 16 621 cm^{-1}. Hence,

$$f(t)=a_R\exp(-t/\tau_R)+a_{L1}\exp(-t/\tau_{L1}) +a_{L2}\exp(-t/\tau_{L2})\,. \quad (12)$$

The convoluted values giving rise to the best fits to the experimental points are shown by open circles in Fig. 2. Decay times of τ_R, τ_{L1}, and τ_{L2} of each component derived from this analysis are summarized in Table I.

The decay time τ_R of the short-lived component is less than 50 ps, which is our time resolution, whereas that of the long-lived component ranges from 0.5 to 1.6 ns depending on ω_i. We list also lifetimes τ_0 of localized exciton luminescence monitored at ω_i, which were determined by decay time measurements under band-to-band excitation. We find that the values of τ_{L1} coincide well with the lifetimes τ_0 of the localized excitons at the frequency ω_i. Thus, the first component showing exponential decay (τ_{L1}) is due to LO phonon-assisted luminescence from localized excitons that are selectively excited at ω_i. Unless the polariton effect is important,[13] a time response of RS is expected to be as short as the duration of the incident pulse, whereas that of luminescence shows an exponential decay. Therefore, the LO_2 line for 16 790 cm^{-1} is due to the resonant luminescence with emission of LO phonon from the localized excitons that are created as a real state at ω_i. When ω_i is decreased from 16 790 cm^{-1}, the Raman component which exhibits the similar time response to the incident pulse appears in addition to the luminescence component and a relative amount of RS component increases. Therefore, we can conclude that the second-order optical process giving rise to the sharp LO_2 lines transforms from resonant luminescence to RRS as a function of ω_i without changing the spectral shape.

Further evidence for the separation of Raman and luminescence components in the decay curves will be given in "time-resolved spectra" shown in Fig. 3. By fixing ω_i constant at 16 702 cm^{-1}, we have measured decay curves as a function of emission frequencies around the LO_2 line. Figure 3 represents "time-resolved" spectra obtained by plotting time-integrated intensities of Raman (■) and resonant luminescence (○) components of observed decay curves as a function of emission frequencies.

TABLE I. Values of decay times obtained from the best fits between the experimental curves and convoluted ones and lifetimes τ_0 of excitons measured by the band-to-band excitation.

Incident frequencies cm^{-1}	τ_R (ns)	τ_{L1} (ns)	τ_{L2} (ns)	τ_0 (ns)
16 833	<0.05	0.50	1.8	0.40
16 817	<0.05	0.50	2.1	0.55
16 790	<0.05	0.85		0.80
16 702	<0.05	1.50		1.45
16 621	<0.05	1.40	6.2	1.50

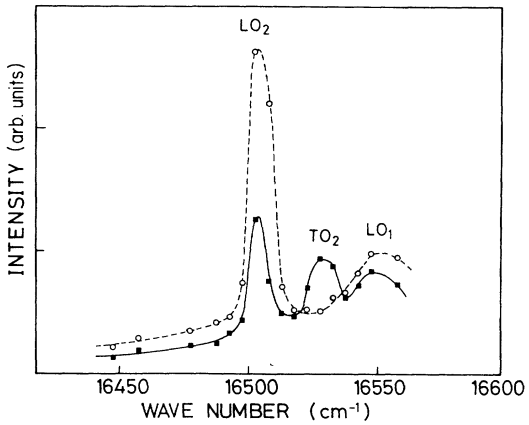

FIG. 3. "Time-resolved spectra" for $\omega_i=16\,702$ cm^{-1} at 1.8 K. Time-integrated intensities of Raman (■) and luminescence (○) components derived from the decay curves are plotted as a function of emission frequencies. Both sets of lines are to guide the reader's eye.

The spectrum for Raman component shows three peaks at the positions of the LO_1, TO_2, and LO_2 lines, whereas that of luminescence component shows two peaks at the positions of the LO_1 and LO_2 lines. Note that the spectral shape of each line is similar for both components within our spectral resolution. This spectral feature reflects the properties of the resonant intermediate state in the second-order optical process in mixed semiconducting crystals; the exciton state is more or less localized depending on exciton frequencies and shows little spectral diffusion so long as the exciton frequency is below the mobile exciton band. Consequently, the luminescence process resonant with such excitons preserves the energy correlation between incident and scattered photons, though the phase correlation is lost. Therefore, the luminescence process and the Raman process, which preserves the correlation in both energy and phase processes, give the same spectral shape. This result confirms that the sharp LO_2 line can be resolved into Raman and resonant luminescence components only by the time-resolved spectroscopy, and also that the continuous transition from luminescence into RS occurs without changing the spectral shape.

It is worthwhile to mention the origin of the second luminescence component with decay time of τ_{L2}. The relative amount of this component in the decay curve becomes larger when ω_i is decreased. The time-integrated intensity of this component as a function of emission frequencies around the LO_2 line gives a broad background spectrum instead of the sharp line. Therefore, this is due to the background luminescence which is not directly related with the resonantly excited excitons. [See spectra (b), (c), and (f) of Fig. 1.]

We briefly discuss the different behavior of the TO_2 line in "time-resolved spectra." The TO_2 line is observed in the "Raman spectrum" while it is not observed in "luminescence spectrum." When ω_i is decreased at 16 621 cm^{-1}, we see the TO_2 line being comparable to the intensity of LO_2 line in time-integrated spectrum (f) in Fig. 1.

The time response measured at this frequency revealed that the Raman component is dominant in the LO_2 line of spectrum (f). Therefore, these results suggest that TO phonon scattering is more enhanced in the Raman process than in the luminescence process. We know also that the intensity of the LO phonon sideband of exciton luminescence is much larger than that of the TO phonon sideband in II-VI semiconductors. The exciton-LO phonon interaction is "forbidden" Fröhlich type, whereas the exciton-TO phonon interaction is allowed deformation type. Consequently, the different type of interaction between excitons and optical phonons is responsible for the enhancement of TO phonon scattering in the first-order Raman process.[14]

V. DISCUSSIONS

A. Intensity ratio

How the intensity ratio between Raman and luminescence components varies with an off-resonance frequency Δ_c is of interest, because this would give evidence of the memory effect of reservoir. Figure 4 represents the ratio of the resonant luminescence intensity to the total emission intensity (a sum of RS and resonant luminescence intensities) as a function of ω_i. The intensities were determined from the time integration of each component of the decay curves. The intensity ratio at 1.8 K shown by open circles is almost unity for $16\,730 < \omega_i < 16\,800$ cm^{-1}, and it decreases sharply in the range where $16\,680 < \omega_i < 16\,730$ cm^{-1}. We should especially note that the ratio exhibits the gradual decrease even at large off-resonance frequency ($\omega_i < 16\,680$ cm^{-1}).

The decrease in the intensity ratio near the X band ($\omega_i \geqq 16\,830$ cm^{-1}) is interpreted in terms of the spectral diffusion; when ω_i is tuned in the vicinity of the X band, a broad luminescence band (denoted by a star in Fig. 1), which is the LO_2 phonon side band of localized exciton luminescence, is observed below the LO_2 line. Since the exciton state is mobile in this frequency region, resonantly excited excitons are effectively transferred to the tail state to be localized.[9,15] Therefore, the large fraction of the luminescence process loses the energy correlation as well as the phase correlation between incident and scattered photons. If we plot the intensity ratio of luminescence, including the nonresonant luminescence to the total secondary emission shown in Fig. 4 by triangles, we find that this ratio is almost unity near the X band. This confirms that the second-order optical process in this region of ω_i is the luminescence process, though the spectral diffusion dominantly occurs.

Before analyzing the experimental ratio of the intensity on the basis of the theory for the resonant second-order optical process, we define a resonance frequency ω_0. In a previous paper (Ref. 3) we took the peak frequency of the LE band as the resonance frequency. However, for the following reasons, we adopt the frequency of the mobile exciton, 16 835 cm^{-1} as the new definition of the resonance frequency. First, the detailed analysis of LE and X bands based on the temperature dependence of lifetimes allowed us to conclude that both the X band and LE band originate from intrinsic excitons, though we assigned the X band as the impurity-related luminescence in the previous paper. Second, the variation of Raman intensity with ω_i does not exhibit a peak at the position of the LE band. In Fig. 5, time-integrated intensities of Raman (■) and resonant luminescence (○) components are plotted as a function of ω_i. We find that the Raman intensity increases when ω_i approaches the X band and it exhibits a maximum at $\sim 16\,820$ cm^{-1}. It is better to discuss the resonant behavior on the basis of the Raman cross section which is corrected with the absorption coefficient, since the Raman cross section shows more clearly an enhancement when ω_i resonates with an intermediate state of the second-order optical process. We tried to measure the absorption coefficient in the range of X and LE bands. Un-

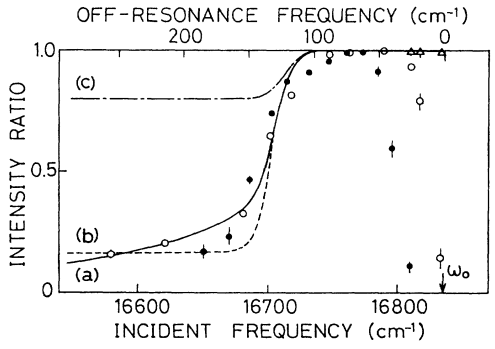

FIG. 4. Intensity ratio of luminescence to total secondary emission in the LO_2 line as a function of incident frequencies and off-resonance frequencies. ○, 1.8 K; ●, 14 K. △ represents the intensity ratio including nonresonant luminescence. Error bars are indicated by a vertical line if they are larger than the open circle. Curve a is the best-fitted curve to the open circles. See text for curves b and c.

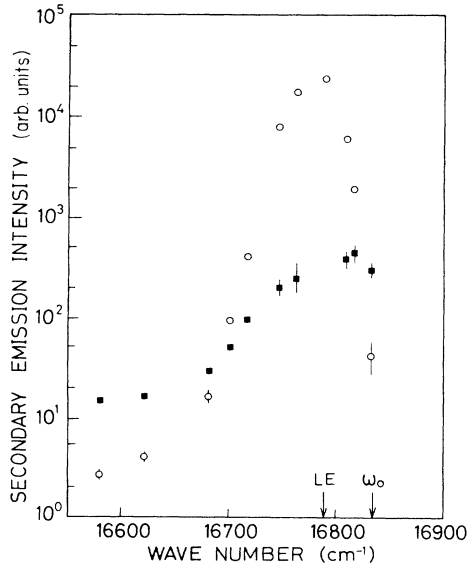

FIG. 5. Secondary emission intensities of Raman and resonant luminescence components as a function of ω_i. Time-integrated intensities of each component were determined from the decay curves at ω_i's. ■, Raman component; ○, resonant luminescence component.

fortunately, however, we could not determine the correct absorption coefficient around the X band because of the strong absorption of light. Nevertheless, the observed absorption spectrum qualitatively shows that the optical absorption increases largely near the X band without exhibiting a peak at the LE band. Therefore, it is reasonable to conclude that the resonant intermediate state in our system is not the state located at the LE band but the state at the X band. Since we could not determine the exact position of the resonance frequency from the resonant enhancement of the Raman intensity, we take the peak position 16 835 cm^{-1} of the X band as the resonance frequency ω_0. The ambiguity of about 10 cm^{-1} exists for this determination of ω_0. We put an off-resonance frequency $\Delta_c=\omega_0-\omega_i$ on the upper abscissa of Fig. 4. As mentioned before, the rapid decrease of the resonant luminescence intensity above the peak position of the LE band is due to the increase in the spectral diffusion because of the weak localization.[16] In this frequency range where the exciton energy approaches the effective edge for the transfer, the activation energy of the localized state becomes very small as discussed in Ref. 9.

B. Theoretical analysis

In what follows, we will analyze the intensity ratio on the basis of the theory taking into account the non-motional-narrowing effect.[7] The ratio $I_L/I_{\rm tot}$ will be calculated from Eqs. (10) and (11) in Sec. II with adjustable parameters of τ_c and $\Gamma=D^2\tau_c$. Γ corresponds to the transverse relaxation rate in the motional-narrowing limit. It is noteworthy that in the limit where $\tau_c=0$, this theory gives the same result as the calculation in the motional-narrowing limit by Mukamel *et al.*,[4] which succeeded to interpret the experimental results of the I_2 vapor system.[1]

The theoretical curve calculated by taking $\gamma^{-1}\sim 1$ ns, $\delta_i\sim 37$ cm^{-1}, $\delta\sim 7.5$ cm^{-1} for the present experiments is shown by a solid line (curve a) in Fig. 4. The best fit between the theoretical curve and the experimental points (open circles) is obtained by choosing $\tau_c=1\times10^{-13}$ s and $\Gamma^{-1}=5\times10^{-10}$ s. If we choose $\tau_c=2.5\times10^{-13}$ s and $\Gamma^{-1}=1\times10^{-10}$ s, the fit is also well within the experimental accuracy.[17] However, if we take $\tau_c=0$, which is the case of the motional-narrowing limit, we could not attain the best fit for any value of Γ. This is shown by the dashed line (curve b) in Fig. 3 for $\Gamma^{-1}=1\times10^{-8}$ s. The significant discrepancy is seen at $\Delta_c>130$ cm^{-1}. We should note that the ratio in the motional-narrowing limit ceases to decrease at large off-resonance, whereas that for $\tau_c\neq0$ continues to decrease. Moreover, if we reduce the value of τ_c to zero, keeping the value of Γ^{-1} fixed at 5×10^{-10} s, the contribution of the luminescence component increases drastically as shown in Fig. 4 by the dash-dotted line (curve c). These results demonstrate that the memory effect of reservoir depresses considerably the luminescence process in the regime where $\Delta_c>130$ cm^{-1}. In this regime, the system cannot stay in its excited state during a time longer than $1/2\pi c\Delta_c=4\times10^{-14}$ s because of the uncertainty relation between energy and time. Therefore, the memory effect due to the finiteness of $\tau_c\sim1\times10^{-13}$ s, i.e., non-motional-narrowing effect, plays a very important role, even if τ_c is much shorter than Γ^{-1}, γ^{-1}, and δ^{-1}. To find this effect, the measurement of off-resonant behavior in this regime is quite important; this is clearly demonstrated in the present study.

In the above analysis, we assumed the radiative lifetime $\gamma^{-1}\sim1$ ns. In our sample, however, the lifetimes vary from 0.4 to 1.4 ns for $\Delta_c\leqq100$ cm^{-1}, and they become constant at 1.5 ns for $\Delta_c>100$ cm. We have calculated the intensity ratio, changing a value of γ^{-1} in order to find out whether the ratio in the range of $\Delta_c\leqq100$ cm^{-1} is sensitive to the value chosen. We have found that it remains approximately unity in this range, even if we change γ^{-1} by an order of magnitude. The ratio is also insensitive to the values of Γ and τ_c as shown by curves a and b of Fig. 4. Consequently, this weak dependence on the values of Γ and γ for $\Delta_c\leqq100$ cm^{-1} is due to the fact that near resonance the dominant process of the second-order process is the luminescence process and the memory effect does not play an important role.

C. Origin of Γ and τ_c: temperature dependence

We now discuss the physical origin of τ_c and Γ in the exciton system in mixed semiconducting crystals. There are two possible mechanisms for the relaxation process in the intermediate state: the exciton scattering by acoustic phonons and that by randomly fluctuated potentials in mixed crystals.[8] The transverse relaxation by the former mechanism is strongly temperature dependent. The relaxation rate Γ due to the exciton scattering by acoustic phonons increases more than one order of magnitude between 1.8 and 14 K, so that the intensity ratio should change significantly with the temperature. To investigate the temperature variation, we have performed the same kind of experiments at higher temperatures. The ratio measured at 14 K is illustrated by solid circles in Fig. 4. It is found that the temperature dependence of the observed intensity ratio between 1.8 and 14 K is weak at $\Delta_c>60$ cm^{-1}.[18] The parameters Γ and τ_c that give the best fit between the experimental points at 14 K and the theoretical curve are $\Gamma^{-1}\sim8\times10^{-10}$ s and $\tau_c=1\times10^{-13}$ s, respectively. In making this fit, we shifted ω_0 towards the lower frequency by an amount of 5 cm^{-1} which corresponds to the decrease in the band gap at 14 K. In contrast to the theoretical estimate of the scattering rate by acoustic phonons, the value of Γ decreases within a factor of 2 between 1.8 and 14 K. Therefore, the acoustic phonon scattering is ruled out as the dissipative process in the intermediate state.

On the other hand, the scattering by randomly fluctuated potentials should be the dominant relaxation process in the exciton system at the low temperature in $A_xB_{1-x}C$ mixed crystals. Since the large number of atomic sites are included inside the Bohr radius of an exciton ($a_0\sim60$ Å), the random distribution of site energy causes the phase randomization, i.e., dephasing. Thus, a coherent exciton for the instant of a pulse excitation loses its phase memory as time goes on. In this case, τ_c is determined by the bandwidth of excitons in the presence of potential fluctuations for a weakly localized exciton or by the width of potential fluctuations for a strongly localized exciton.

Both energies are thought to be of the order of the width of inhomogeneous broadening (~ 37 cm^{-1}). This value is close to the value of $1/2\pi c\tau_c$ (~ 53 cm^{-1}) for $\tau_c = 1 \times 10^{-13}$ s that is given by the best fit in Fig. 4 (curve *a*). Therefore, it is reasonable to conclude that the exciton damping of our system at low temperatures arises from the random potential fluctuations.

A slight decrease of Γ at higher temperature is interpreted in terms of the decrease in localization; since the phonon-assisted transfer of excitons between random potential wells increases at elevated temperature, the potential fluctuations which excitons see are depressed. Therefore, Γ due to the exciton damping by the randomly fluctuated potentials should be decreased at higher temperature.

VI. CONCLUSIONS

We have studied the transient behavior of secondary emission associated with localized excitons in $Cd_xZn_{1-x}Te$ mixed crystals in the wide range of the off-resonance frequency. Time-resolved spectroscopy revealed the continuous transition from luminescence to RS as a function of ω_i without changing the spectral shape. The observed intensity ratio between Raman and luminescence components has been analyzed by the theory considering the finiteness of the correlation time for phase fluctuations of an exciton due to the randomness. In spite of the simplified model, we have found that the observed ratio in the wide range of Δ_c is unambiguously explained by this theory; this provides evidence for the importance of the non-motional-narrowing effect in the second-order optical process. This non-motional-narrowing effect should be generally seen in the off-resonance regime in the second-order optical process of the various systems in vapor and solids. It is also noted that this effect leads us to natural understanding of the continuous transition from luminescence in the resonant case to ordinary RS in the far off-resonance case.

ACKNOWLEDGMENTS

This work was supported in part by the Scientific Research Grant-in-Aid No. 58540163 from the Ministry of Education, Science and Culture of Japan. The work of M.A. was performed while at the Institute for Solid-State Physics, The University of Tokyo, 7-22-1 Roppongi, Minato-ku, Tokyo 106, Japan.

---

*Present address: Department of Applied Physics, Faculty of Engineering, Nagoya University, Chikusa-ku, Nagoya 464, Japan.

[1]P. F. Williams, D. L. Rousseau, and S. H. Dworetsky, Phys. Rev. Lett. **32**, 196 (1974).

[2]T. Kushida, S. Kinoshita, F. Ueno, and T. Ohtsuka, J. Phys. Soc. Jpn. **52**, 1835 (1983).

[3]A. Nakamura, M. Shimura, M. Hirai, and S. Nakashima, Solid State Commun. **52**, 583 (1984).

[4]S. Mukamel, A. Ben-Reuven, and J. Jortnor, Phys. Rev. A **12**, 947 (1975).

[5]T. Takagahara, E. Hanamura, and R. Kubo, J. Phys. Soc. Jpn. **43**, 1522 (1977).

[6]M. Aihara and A. Kotani, Solid State Commun. **46**, 751 (1983).

[7]M. Aihara, Solid State Commun. **53**, 437 (1985).

[8]M. Aihara, Phys. Rev. Lett. **57**, 463 (1986).

[9]A. Nakamura, M. Shimura, M. Hirai, and S. Nakashima, Proccedings of the 5th International Conference of Dynamical Processes in Excited States of Solids, Lyon, 1985 [J. Phys. (Paris) Colloq. **46**, C7-179 (1985)].

[10]In contrast to the assignment of bound excitons in $Cd_xZn_{1-x}Te$ by E. Cohen, R. A. Street, and A. Muranevich [Phys. Rev. B **28**, 7115 (1983)], this assignment has been found to be more adequate in our crystal from the experimental results of temperature and excitation frequency dependence of exciton dynamics (Ref. 9). The main difference may result from the different composition ratio of the samples studied: their samples are near the end crystal ($x > 0.9$) whereas $x = 0.32$ in our sample.

[11]For localized excitons in CdS_xSe_{1-x}, e.g., see S. Permogorov, A. Reznitskii, S. Verbin, G. O. Muller, P. Flogel, and M. Nikiforov, Phys. Status Solidi B **113**, 589 (1982).

[12]For localized exctions in $GaAs_{1-x}P_x$, e.g., see S. Lai and M. V. Klein, Phys. Rev. Lett. **44**, 1087 (1980).

[13]The width of inhomogeneous broadening of excitons δ_i is estimated to be ~ 37 cm^{-1} from the lower-energy tail of the absorption below the *X* band. This value is much larger than the longitudinal-transverse splitting [< 10 cm^{-1} in both end crystals], so that we can neglect the polariton effect.

[14]R. Martin, Phys. Rev. B **4**, 3676 (1971).

[15]The exciton transfer to the tail state is also observed in CdS_xSe_{1-x}. J. A. Kash, A. Ron, and E. Cohen, Phys. Rev. B **28**, 6147 (1983).

[16]Time-resolved spectra measured under the band-to-band excitation gave us some information about the form of the density of state. At an early stage of time delay, only the *X* band is observed and then the LE band appears. When the time elapses, the intensity of the *X* band decreases rapidly and the peak position of the LE band shifts towards the lower-frequency side across the peak position of the LE band of the time-integrated spectrum. This result indicates that the density of state does not have a peak at the position of the LE band, although there exists "a mobility edge of excitons." We think that the density of states in the tail state decreases monotonically like an exponential function as studied for the case of CdS_xSe_{1-x} by E. Cohen and M. D. Sturge [Phys. Rev. B **25**, 3828 (1982)]. We should notice that in CdS_xSe_{1-x} luminescence from mobile excitons was not observed. Considering the fact that the mobility edge does not exist in this case (Ref. 15), observation of the *X* band may arise from the existence of the mobility edge.

[17]In this analysis we took 16 835 cm^{-1} as ω_0 together with $\delta_i \sim 37$ cm^{-1}. The width at which the intensity ratio becomes 0.5 is mainly determined by the inhomogeneous broading δ_i. If we take 16 820 cm^{-1}, which is the peak position of the Raman intensity, δ_i is also estimated to be a smaller value (~ 31 cm^{-1}). As a result, the fit is also well for almost the same values of τ_c and Γ^{-1}.

[18]At $\Delta_c < 60$ cm^{-1}, we notice that the spectral diffusion is more pronounced at higher temperature.